PROCEEDINGS OF SPIE

SPIEDigitalLibrary.org/conference-proceedings-of-spie

# Generation of surface shape from variable-resolution video moire contours

Joel H. Blatt
Scott Christian Cahall
Bernard R. Gilbert
Jeffery A. Hooker
Gary L. Wallace

SPIE.

# Generation of surface shape from variable resolution video moiré contours

Joel H. Blatt (blatt@pss.fit.edu), MEMBER SPIE
Scott C. Cahall, MEMBER SPIE
Bernard Gilbert
Jeffery A. Hooker, MEMBER SPIE
Gary L. Wallace

Florida Institute of Technology, Physics and Space Sciences Department
150 West University Blvd., Melbourne, FL 32901-6988

## ABSTRACT

Several methods for generation of three dimensional surface shapes from variable resolution video moiré contours are described. In a classical moiré system, a physical grating is projected on a target and also used to view the target. The moiré contours are generated in the plane of the viewing grating. An unambiguous surface shape can then be computed by processing a series of moiré images where the grating, target, or both are moved. By using an interferometer to generate and project variable pitch gratings and video technology to generate the moiré contours, a 3-D surface can be scanned at different resolutions and used on a wide range of object sizes. The elimination of the physical grating also leads to surface generation techniques that do not use moving parts, increasing reliability. From these video moiré contours, it is possible to uniquely reconstruct the 3-D surface, making the distinction between concave and convex surfaces. In one technique, a computer is used to mix digitized images of distorted gratings projected on the object with computer generated gratings, creating the moiré patterns. By shifting one grating, it is possible to reconstruct the surface without having to move the object being scanned.

## 1. INTRODUCTION

We have developed a variable resolution video moiré system whose zoom capability allows inspection of a wide range of objects with resolution adjustable to fit the object and inspection task[1,2,3,4]. A tilted mirror Michelson interferometer illuminated with an Argon-ion laser generates variable spacing gratings which are projected onto a target and a flat reference surface as shown in Fig. 1. A high resolution video camera uses the reference grating image to chroma-key filter the image of the distorted grating seen on the target by a second video camera. If the reference surface is replaced by a perfect target, difference or error map moiré contours between the master and test target are generated in real time. Tilting the interferometer mirror makes it possible to change the depth resolution of the moiré contours in real time. This paper describes generation of surface shape from variable resolution moiré.

## 2. MOIRÉ GENERATION

By mixing a perfect grating with a distorted grating, moire patterns are generated. The moiré pattern can be represented by

$$g(x,y) = a(x,y) + b(x,y)\cos[\phi(x,y)] \qquad (1)$$

where a(x,y) and b(x,y) are unwanted variations in the intensity from nonuniform projection or reflection of the light and $\phi(x,y)$ is the phase of the moiré pattern's fringes which contains the height information. After the grating noise is removed from the moiré, the phase of each location needs to be determined. This phase information is represented by $\phi(x,y)$ in Eq. (1), and when unwrapped provides a scaled version of the surface shape. Various methods are used to generate the moiré patterns from a surface.

Classical shadow moiré topography uses a light source projected through a grating at an angle onto an object. The object is viewed through the same grating by a camera that is at a different angle[5]. The grating is then translated in its plane to average out the gratings from the shadow moiré pattern. To shift the moiré fringes to determine the surface curvature, the object is translated normally to the grating in a precisely controlled manner. This can cause problems with an increase in object size and is not desirable in an industrial inspection system where precise movement of the object may be impractical.


0-8194-1022-5/93/$4.00

In projection moiré topography a regular grating is projected onto an object at an angle and viewed through a second physical grating at a different angle. This generates a moiré pattern that can be separated from the grating pattern by the use of an FFT routine[6]. The moiré pattern typically has a frequency between the lower frequency nonuniform light reflection from the object and the higher frequency of the grating. After the FFT the moiré frequencies are separated and translated to center around the origin before the inverse Fourier transform is used to obtain $\phi(x,y)$ in Eq. (1). In certain cases the moiré pattern and grating frequencies or the moiré pattern and nonuniform light reflection frequencies may cross each other and cause problems in the separation procedure and the physical grating again has to be moved to obtain another moiré pattern with the fringes shifted before the direction of the surface curvature can be determined and the surface shape can be calculated. The projected grating can also be translated by the use of a piezoelectric transducer (PZT) mounted to a mirror. This simply replaces one moving part, the physical grating, with another moving part, a mirror.

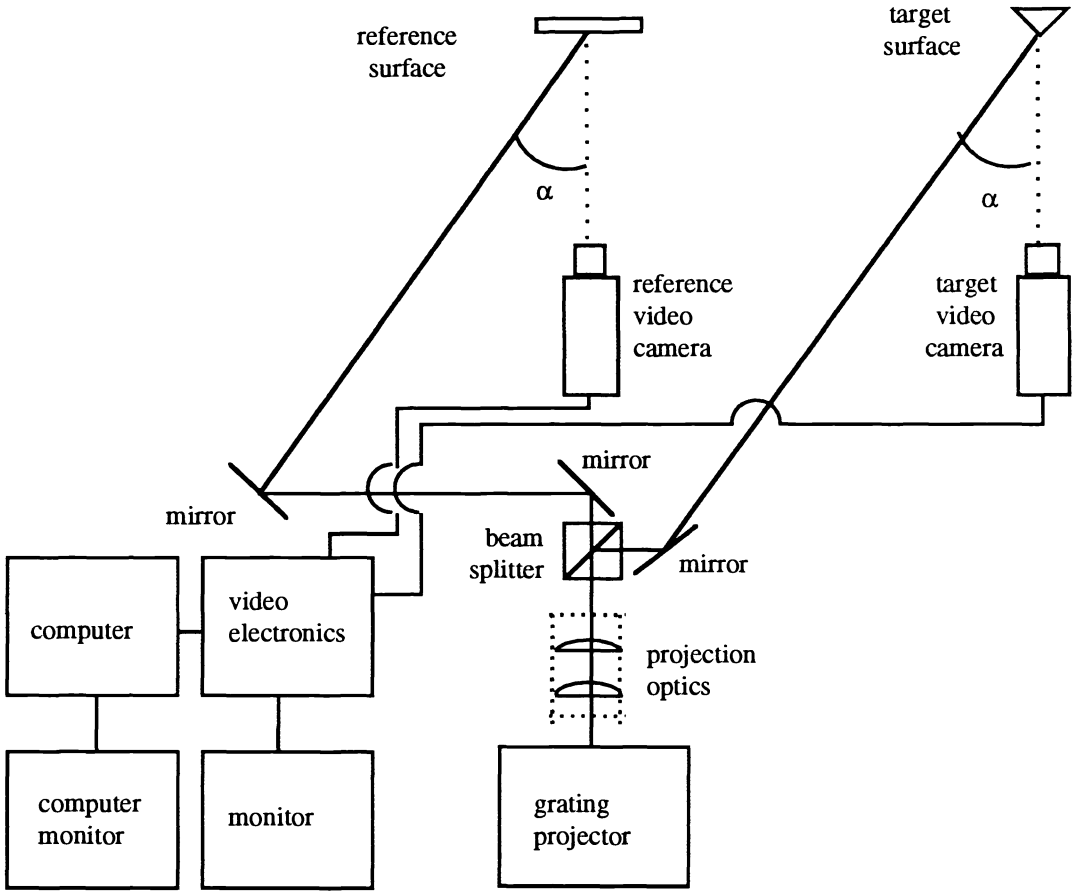


Fig. 1. Video Moiré System

To eliminate as many moving parts as possible video moiré is used. A grating is projected onto the test object at an angle and viewed by a camera at a different angle. Typically the camera is positioned normal the the surface that is to be examined. A beamsplitter allows the same grating to be projected onto a flat surface, or onto a "perfect" object for error surface determination. This forms a reference grating that is viewed by a second camera. The two video signals are then combined in a video mixer to form the moiré pattern. The two grating beams can be translated by an acousto-optic cell to average out the gratings[3,7]. Another acousto-optic cell can be used to translate only the reference beam and shift the moiré fringes in a precise manner. This allows the surface to be determined by a system that has no moving parts. By adding variable tilt to the interferometer and zoom lenses on the cameras, moving parts are added to the system but the additions increase the flexibility of the system greatly.

## 3. GENERATION OF THE SURFACE SHAPE

To generate the surface from the moiré patterns, the term $\phi(x,y)$ in Eq. (1) must be determined. The minimum number of moiré patterns needed to determine $\phi(x,y)$ is two. If two patterns are used, a shift of $\pi/2$ is needed between the moiré fringes and $a(x,y)$ must be eliminated by the use of an FFT and low pass filtering of the frequencies. After $a(x,y)$ is eliminated from the two moiré patterns and the moiré patterns frequencies are shifted to average zero, the two patterns can be divided to obtain

$$\phi(x,y) = \tan^{-1} (-I_2/I_1), \qquad (2)$$

where $\phi(x,y)$ is the phase information of the first, unshifted, image[8]. In our experiment, the $a(x,y)$ could not be reduced enough to eliminate the need for the FFT and filtering. The FFT and filtering adds extra computing time and causes problems if the frequencies of $a(x,y)$ overlap the frequencies in the moiré patterns.

To eliminate the need for the FFT, three moiré patterns can be used. Eq. (1) has three unknown terms, $a(x,y)$, $b(x,y)$, and $\phi(x,y)$. To solve for any one of these terms specifically, three images are needed. A shift of $-\pi/3$, 0, $\pi/3$ is used between the moiré fringes in the three images[9]. The surface can then be found from

$$\phi(x,y) = \tan^{-1} (((\text{sqrt}(3)/2)(-I_1+I_3))/(I_2-0.5I_1-0.5I_3)). \qquad (3)$$

This method was successfully used to determine the surface of a test object, but it was observed that small variations from the $\pi/3$ shifts between images caused large errors in the phase information. This gave smooth surfaces a stepped appearance, one step for each moiré fringe, if the shifts were not precisely $\pi/3$.

A self-calibrating algorithm that can calculate the actual phase shifts between images requires four images with three equal phase shifts between them, $-3\beta$, $-\beta$, $+\beta$, $+3\beta$[10]. Four phase shifts between the images gives us the following formulas,

$$\tan^2\beta = ((3I_2-3I_3-I_1+I_4)/(I_1+I_2-I_3-I_4)) \qquad (4)$$

$$\tan^2\phi = ((3I_2-3I_3-I_1+I_4)(I_1+I_2-I_3-I_4)/(I_1-I_2-I_3+I_4)). \qquad (5)$$

This gives the $\tan^2$ of $\phi(x,y)$ instead of tan of $\phi(x,y)$ and allows the numerator and denominator of (4) and (5) to go the zero at the same time. These problems can be eliminated with five phase shifts.

With a five phase shift method where the fringes are shifted $\pi/2$ each time, $-\pi$, $-\pi/2$, 0, $+\pi/2$, $+\pi$, the phase can be calculated from

$$\phi(x,y) = \tan^{-1} (2(I_2-I_4)/2I_3-I_5-I_1). \qquad (6)$$

This also does not allow the numerator and denominator to go to zero at the same time and has small phase errors when the phase shift is not exactly $\pi/2$[10]. For these reasons the five phase shift technique was used in two methods that reconstruct the surface, spatial phase stepping with one distorted grating and for the five shifted moiré images. Simple arithmetic on the intensity values, an arctan calculation and an unwrapping routine will supply a scaled version of the height information at every pixel position.

The spatial phase stepping method[11] calculates the phase by taking the value of a pixel, a pixel $\pi/2$ phase ahead, a pixel $\pi$ phase ahead, a pixel $\pi/2$ phase behind, and a pixel $\pi$ phase behind the first pixel. To find the number of pixels to equal the $\pi/2$

and $\pi$ shifts, the average pitch of the gratings over the entire image was calculated and used. Since pixels ahead and behind of each pixel whose phase is to be determined are needed, the pixels up to a $\pi$ phase shift from the top and bottom (for gratings projected horizontally, the left and right side for gratings projected vertically) of the image do not have their phase calculated. The moiré method uses five separate images, shifting the phase of the entire image by $\pi/2$ each consecutive image taken. These images can be made with a video chroma key or a computer generated grating being digitally combined with a distorted grating image.

## 4. EXPERIMENTAL RESULTS

Using the setup in Fig. 1, it is easy to determine 3-D surfaces of different size smooth surfaces. The variable pitch of the interferometer allows gratings with a pitch of less than a millimeter to larger than a centimeter to be projected onto the test surface and reference surface. This allows the resolution in the z axis (normal to the surface) to be varied greatly. The focal depth of the camera, camera resolution, and steepness of the surface also limit the z resolution of the system. Our system allows for height differences of about 0.1 mm to be resolved. The zoom lens and video cameras control the x and y resolution of the system. Our system can be zoomed in on an object to have a x and y resolution of about 0.1 mm. The laser intensity also limits the size of the object to be scanned by not being bright enough to project a detectable grating onto an extremely large object. With the 100mW Argon-ion laser used in our system, we can easily scan object larger than 40cm x 40cm.

To demonstrate the resolution of the system, the surface of a quarter was scanned. Before the grating was projected onto the quarter, the surface of the quarter was lightly coated with flat white paint to allow for a diffuse reflection. The surface in Fig. 2b and c was then determined from the distorted grating in Fig. 2a. This method was used since this only required one nonaveraged image and was much faster than multiple moiré method.

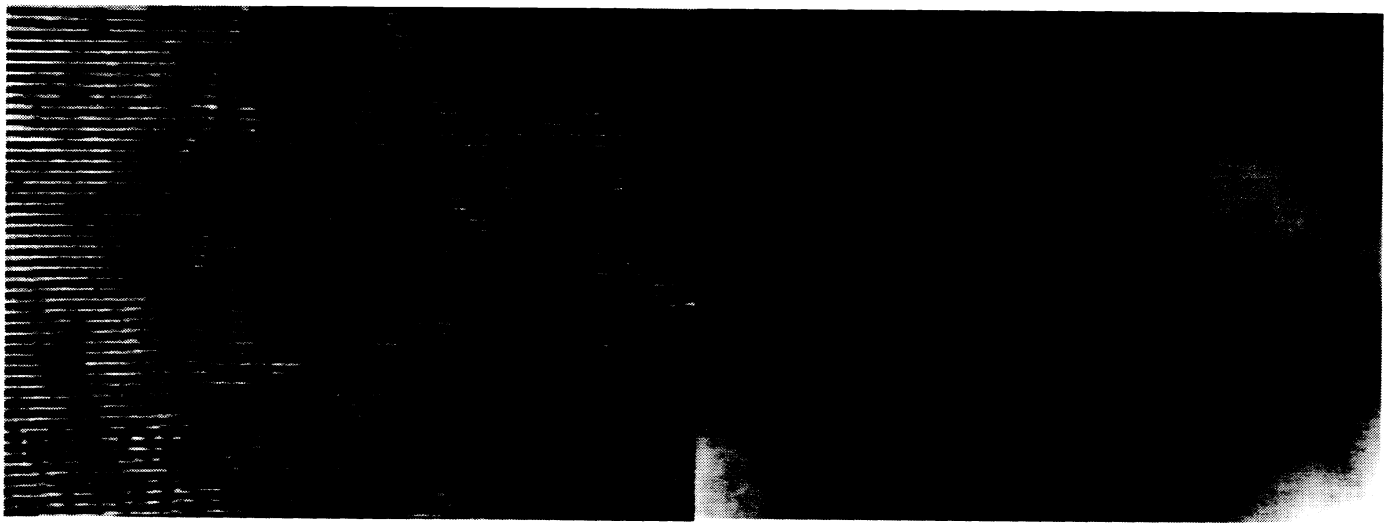

Fig. 2a. Grating projected on a quarter

Fig. 2b. Surface of a quarter (brightness $\alpha$ height)

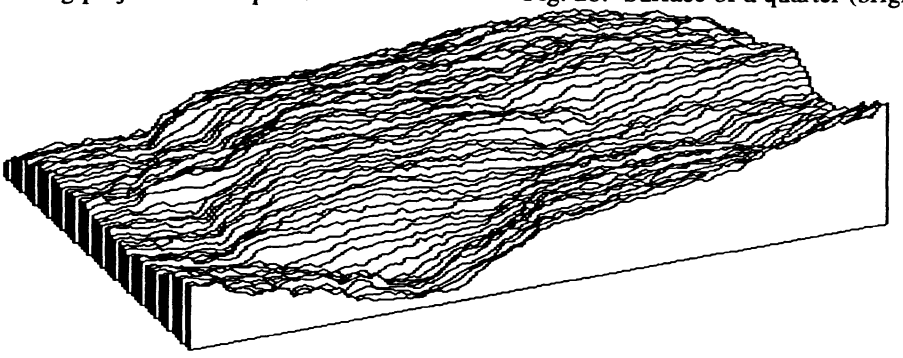

Fig. 2c. Wireframe surface of quarter

A mask that is 5cm wide, 3cm high, and 2cm in depth was used as a typical example of an object that the system could scan. Fig. 3b-f show the moiré patterns with a $\pi/2$ phase shift between them. The phase shift was made by moving the reference camera producing a shift in the reference gratings. This shift will be accompliced with an acousto-optic cell in the reference beam in the future. The images are also averaged while both projected gratings are shifted to help average out the gratings[7]. This was done by moving a beam steering lens and will be done with an acousto-optic cell in the future to eliminate the need to move these parts of the system. The phase is then calculated from Eq. (6) and seen in Fig. 3g. This is the phase of the third moiré image and can be unwrapped to form the surface seen in Fig. 3h. Fig. 4 shows the wireframe surface calculated for the mask. If a higher x and y spatial resolution is needed, the system can easily zoom in on an area of the mask and reconstruct the surface again. If the z resolution needs to be increased, the pitch of the gratings can be reduced.

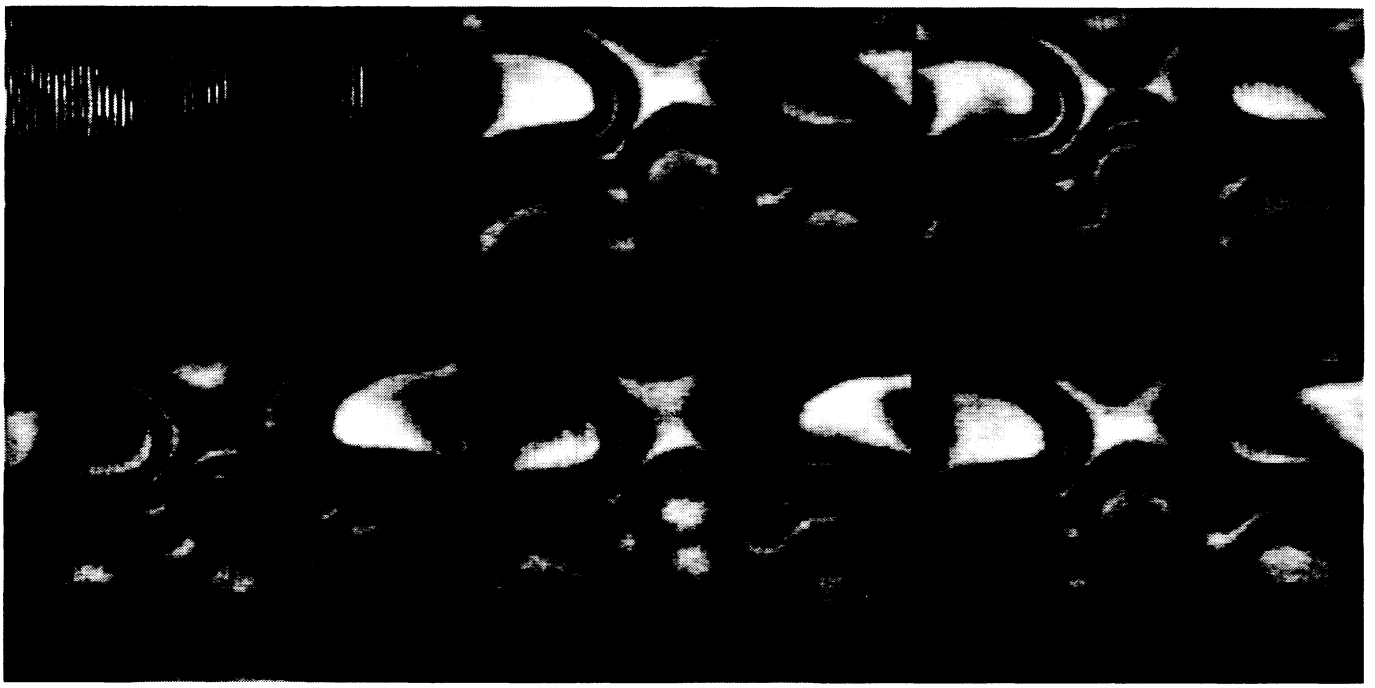

Fig. 3a. Gratings projected onto a mask.

Fig. 3b-f. Moiré contours of the mask

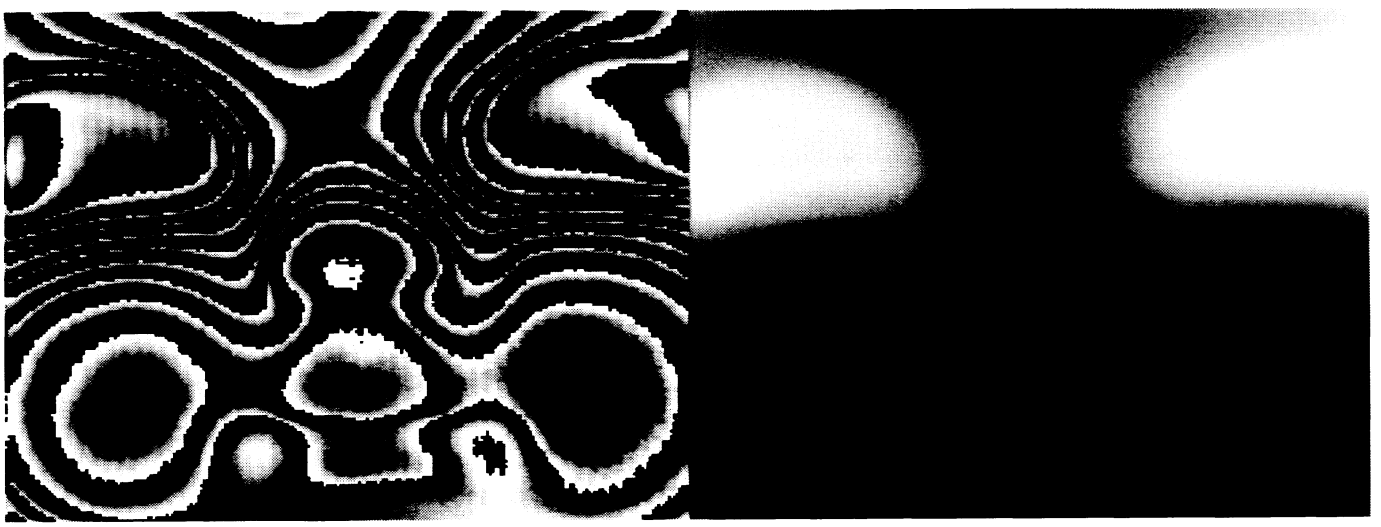

Fig. 3g. Phase information from the moiré contours

Fig. 3h. Surface of the mask (darkness $\alpha$ height)

The moiré patterns can be generated in the computer using just the grating image. This allows precise control over the shift of the reference grating. Fig. 5 shows three moire images generated from the distorted grating image (Fig. 3a). The second image has a $\pi/3$ shift from the first image and the third image has a $2\pi/3$ shift from the first image. The surface can then be generated from the computer moiré, giving a second method that only requires one image. The disadvantage to generating the moiré in the computer is time. For example, averaging out the grating in the computer moiré takes more computing time than generating the entire surface using the spatial shift method.

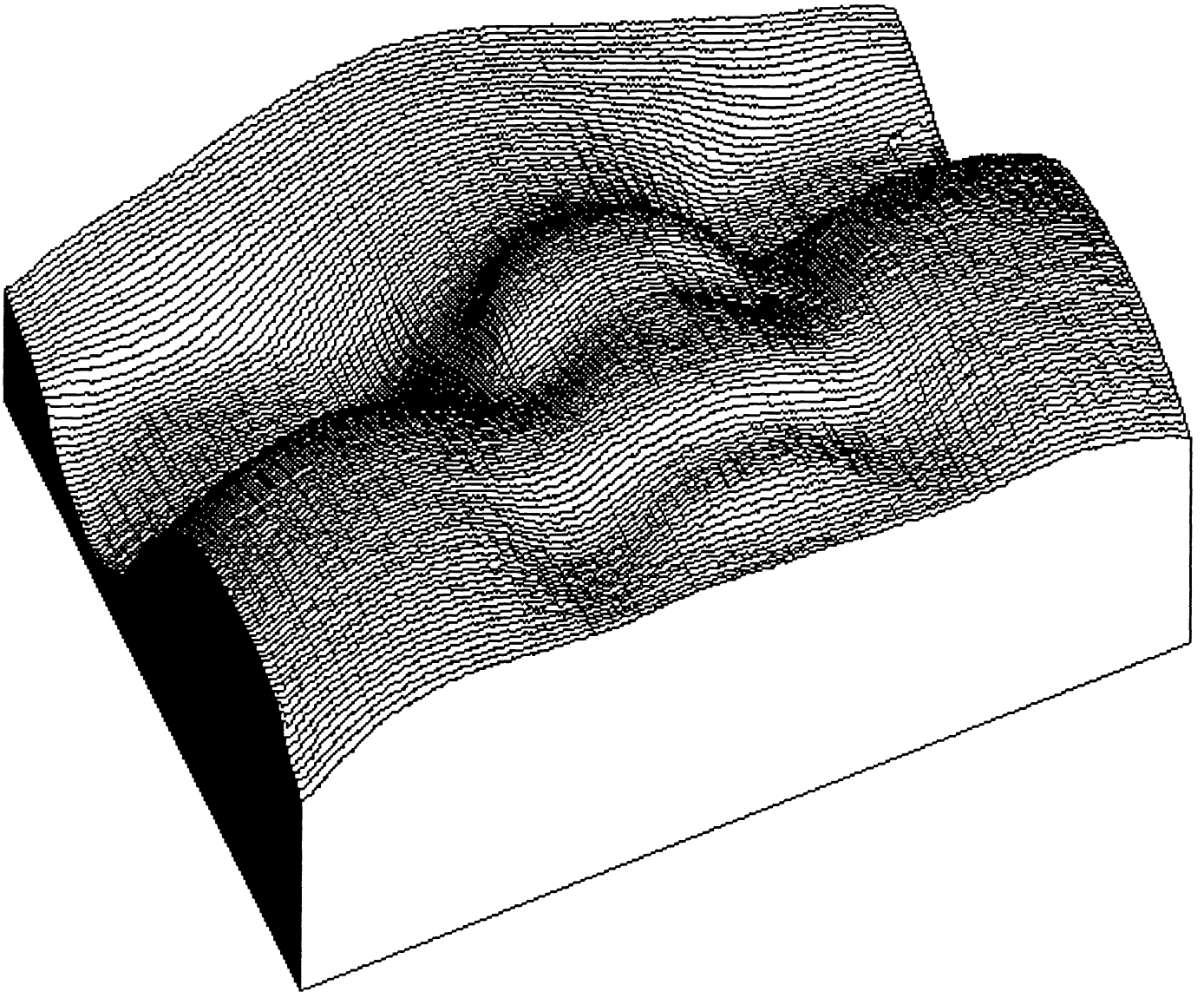

Fig. 4. Wireframe surface of mask

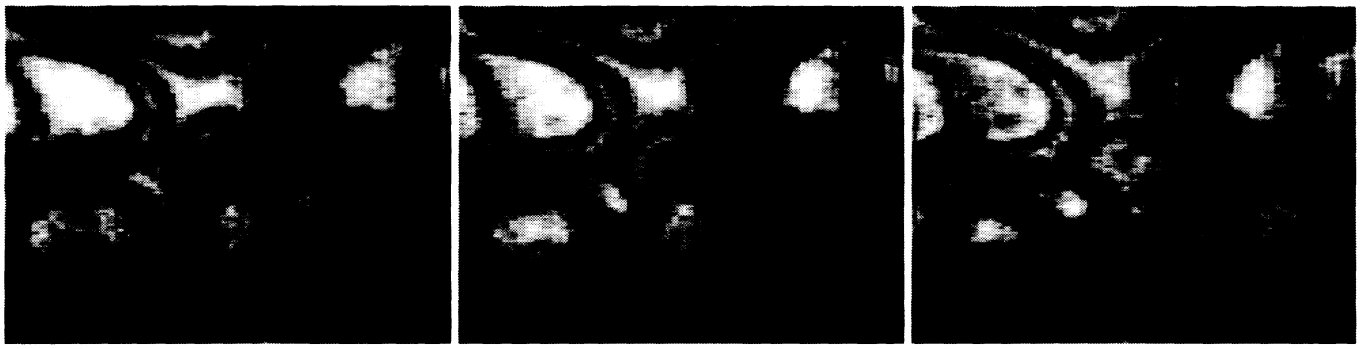

Fig. 5. Computer generated moiré

The system can also be used to test surfaces against a "perfect" surface by using just the projected gratings on the "perfect" surface and on the test surface or the moiré pattern between the surfaces. Projected gratings on a "perfect" pipe can be seen Fig. 6a. A pipe with a dent has the same grating projected onto it in Fig. 6b. The error surface, seen in Fig. 6c, is then calculated from the difference between the two surfaces. This surface is the test object's, the dented pipe's, surface displacement from the correct position, reference pipe's surface, at each of pixel location. The error surface determination from just projected gratings is faster because only two nonaveraged images are used. The reference, or "perfect" object, image can be reused if several tests are being made, reducing the images needed to one per test after the "perfect" object is scanned. The disadvantage of this method is that it needs near perfect alignment. For setups that have the test objects at known positions to a high tolerance of accuracy this alignment would not cause difficulties. Difficulties occur when doing the alignment by hand since the feedback of the error surface is not in realtime.

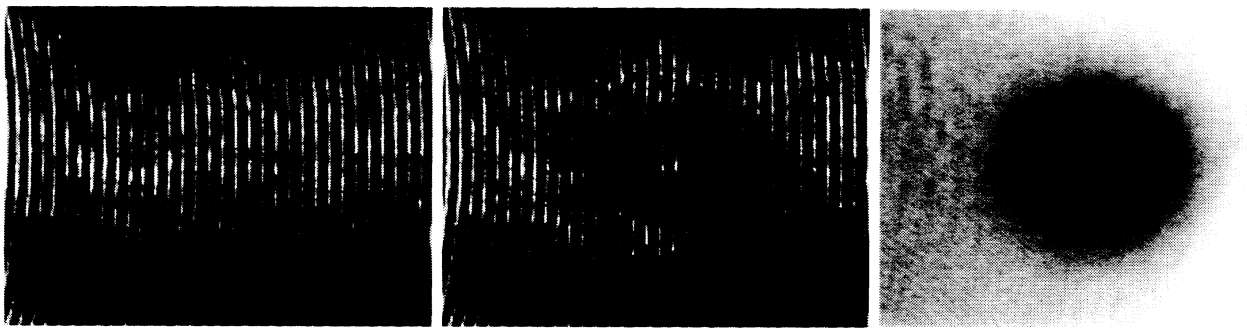

Fig. 6a. Grating on a reference pipe b. Grating on a dented pipe c. Error Map

By using the real time moiré contours the system can produce, alignment of the surface is made easier. With the realtime feedback, the alignment can be done by hand but the processing takes longer because five images are used. The two methods of error surface construction can be combined by using the real time moiré to align the object and the grating images for the calculations. The setup we use allows large areas to be scanned, identifying the areas that have imperfections. Once these areas are identified, the resolution of the system can be increased to better examine each flaw area.

## 5. CONCLUSION

We have demonstrated three method to generate surface shape from variable resolution video moiré. All methods are adaptable for use in an inspection system with no moving parts. The first method generates the shape from 5 phase shifted moiré images where the phase shifts can be performed by an AO cell moving the reference grating. The second method generates the phase shifts and the surface from a single image of the target under structured illumination. A third method generates the moiré images in the computer from a single image of the target under structured illumination. The first two methods have the least computation time.

*Acknowledgements*

This research was sponsored by grants from the State of Florida, the Newport Corporation, and NEOS Technologies, Inc.

*References*

1. J.H. Blatt, J.A. Hooker, E.H. Young and R.V. Belfatto, "3-D Inspection of Large Objects by Moiré Profilometry," *Proceedings ICALEO* '89, Vol. 70-Optical Sensing and Measurement, 12, 1989.
2. J.H. Blatt, R.V. Belfatto, J.A. Hooker and E.H. Young, "Video Applications to Moiré Metrology," Journal of Laser Applications, Vol. 2, No. 3 & 4, 35, Summer/Fall 1990.
3. J.A. Hooker, "Video Applications to Moiré Metrology," Ph.D. Dissertation, Florida Institute of Technology, 1991.
4. J.H. Blatt, J.A. Hooker, and F.M. Caimi, "ADAPTATION OF VIDEO moiré TECHNIQUES TO UNDERSEA MAPPING AND SURFACE SHAPE DETERMINATION," requested paper in *Optics and Lasers in Engineering,* **16**, issues 4 & 5, 265-278, 1992.
5. J.J.J. Dirckix, W.F. Decraemer, G. Dielis, "Phase Shift Method on Object Translation for Full Field Automatic 3-D Surface Reconstruction from Moiré Topograms," Applied Optics, Vol. 27, No. 6, 15 March 1988.
6. Mitsuo Takeda, Hideki Ina, Seiji Kobayashi, "Fourier-transform Method of Fringe-pattern Analysis for Computer-based Topgraphy and Interferometry," Journal of Opticial Society of America, Vol. 72, No. 1, January 1982.
7. J.H. Blatt, J.A. Hooker, H.-C. C. Ho, and E. H. Young, "The application of acousto-optic cells and video processing to achieve signal-to-noise improvements in variable resolution moiré profilometry", *Optical Engineering,* **31**(10), 2129-2138 (1992).
8. Guan-Chang Jin, Shouhoug Tang, "Automated Moiré Contouring of Diffuse Surfaces," Optical Engineering, Vol. 28, No. 11, November 1989.
9. Lawrence Mertz, "Real-time Fringe-pattern Analysis," Applied Optics, Vol. 22, No. 10, 15 May 1983.
10. P. Hariharan, B. F. Oreb, and T. Eiju, "Digital Phase-shifting Interfermetry: a simple error-compensating phase calculation algorithm," Applied Optics, Vol. 26, No. 13, 1 July 1987.
11. D.C. Williams, N.S. Nassar, J.E.Banyard, M.S.Virdee, "Digital Phase-step Interferometry: a simplified approach," Optics & Laser Technology, Vol. 23, No. 3, 1991.